





ORIGINAL PAPER

Development of the sympathetic trunks in human embryos

Nutmethee Kruepunga^{1,2}  | Jill P. J. M. Hikspoors¹  | Cindy J. M. Hülsman¹ |
Greet M. C. Mommen¹ | S. Eleonore Köhler¹  | Wouter H. Lamers^{1,3} 

¹Department of Anatomy & Embryology, Maastricht University, Maastricht, The Netherlands

²Department of Anatomy, Faculty of Science, Mahidol University, Bangkok, Thailand

³Tytgat Institute for Liver and Intestinal Research, Academic Medical Center, Amsterdam, The Netherlands

Correspondence

Wouter H. Lamers, Department of Anatomy & Embryology, Maastricht University, Universiteitssingel 50, 6229 ER Maastricht, The Netherlands.
Email: wh.lamers@maastrichtuniversity.nl

Funding information

Stichting Rijp

Abstract

Although the development of the sympathetic trunks was first described >100 years ago, the topographic aspect of their development has received relatively little attention. We visualised the sympathetic trunks in human embryos of 4.5–10 weeks post-fertilisation, using Amira 3D-reconstruction and Cinema 4D-remodelling software. Scattered, intensely staining neural crest-derived ganglionic cells that soon formed longitudinal columns were first seen laterally to the dorsal aorta in the cervical and upper thoracic regions of Carnegie stage (CS)14 embryos. Nerve fibres extending from the communicating branches with the spinal cord reached the trunks at CS15–16 and became incorporated randomly between ganglionic cells. After CS18, ganglionic cells became organised as irregular agglomerates (ganglia) on a craniocaudally continuous cord of nerve fibres, with dorsally more ganglionic cells and ventrally more fibres. Accordingly, the trunks assumed a “pearls-on-a-string” appearance, but size and distribution of the pearls were markedly heterogeneous. The change in position of the sympathetic trunks from lateral (para-aortic) to dorsolateral (prevertebral or paravertebral) is a criterion to distinguish the “primary” and “secondary” sympathetic trunks. We investigated the position of the trunks at vertebral levels T2, T7, L1 and S1. During CS14, the trunks occupied a para-aortic position, which changed into a prevertebral position in the cervical and upper thoracic regions during CS15, and in the lower thoracic and lumbar regions during CS18 and CS20, respectively. The thoracic sympathetic trunks continued to move further dorsally and attained a paravertebral position at CS23. The sacral trunks retained their para-aortic and prevertebral position, and converged into a single column in front of the coccyx. Based on our present and earlier morphometric measurements and literature data, we argue that differential growth accounts for the regional differences in position of the sympathetic trunks.

KEYWORDS

ganglionic cells, nerve fibres, neural crest cells, para-aortic, para-vertebral, primary and secondary sympathetic trunks

This is an open access article under the terms of the Creative Commons Attribution-NonCommercial-NoDerivs License, which permits use and distribution in any medium, provided the original work is properly cited, the use is non-commercial and no modifications or adaptations are made.

© 2021 The Authors. *Journal of Anatomy* published by John Wiley & Sons Ltd on behalf of Anatomical Society

1 | INTRODUCTION

The peripheral autonomic nervous system derives mostly from neural crest cells (NCCs) that arise concomitantly with neurulation in a cranio-caudal gradient at the junction of the neural tube and skin (Pla & Monsoro-Burq, 2018; Theveneau & Mayor, 2012). In human embryos NCCs appear in a cranio-caudal sequence between CS10 and CS15 [29–36 days of development (Kruepunga et al., 2020a; O’Rahilly & Müller, 2007)]. After delamination, these NCCs migrate ventrally to form, among others, dorsal root ganglia, sympathetic ganglia and pre-aortic nerve plexuses (Theveneau & Mayor, 2012; Vega-Lopez et al., 2017). The sympathetic trunks consist of a bilateral chain of ganglia and nerve fibres. Several studies have suggested that the sympathetic trunks and adrenal medulla share a common progenitor and constitute the sympathoadrenal lineage. The migratory route of the NCCs of the sympathoadrenal lineage, and the successive appearance of ganglionic cells and interganglionic nerve fibres of the sympathetic trunks, has been described in mammals, including humans, already a century ago (His Sr, 1890; Kuntz, 1910; Kuntz, 1920; Streeter, 1912). However, the regulation of its putatively metameric configuration was established only relatively recently (Goldstein & Kalcheim, 1991; Groen et al., 1987; Kasemeier-Kulesa et al., 2005). The complex peripheral deployment of neural crest cells to the sympathetic system is often not considered beyond the separation of the sympathoadrenal lineage into sympathetic trunks and adrenal medulla. As a consequence, many schematics illustrating this aspect are reduced to a transverse section of the embryo only (Furlan et al., 2017; Huber, 2006; Lumb & Schwarz, 2015).

An only partially understood topographical aspect of the developing sympathetic trunks is their position relative to the dorsal aortae. The sympathetic trunks form lateral to the aorta. In this para-aortic position, they are known as the “primary” sympathetic trunks. This position changes gradually to one between the aorta and vertebral column (prevertebral), or one lateral to the vertebral bodies (paravertebral). In the paravertebral position the trunks are referred to as “secondary” sympathetic trunks (Gibbins, 1994; Kuntz, 1920). The ganglionic cells of the primary trunks are still mitotically active (Rothman et al., 1978), but have already acquired an aminergic phenotype before their topographical position begins to change to the more dorsolateral prevertebral position (Cochard et al., 1979). The significance of this change in position is still poorly understood. One hypothesis states that the primary sympathetic trunks represent the phylogenetically older structure, from which neurons migrate dorsally to form the secondary sympathetic trunks (Gibbins, 1994). A more recent report showed that shortly after arrival of the primary sympathetic trunks at the lateral side of the aorta, brain-derived neurotrophic factor (BDNF) secreted by approaching preganglionic nerve fibres in the spinal nerves induces the primary sympathetic ganglia to re-migrate dorsally (Kasemeier-Kulesa et al., 2015). Both accounts emphasize the importance of the different topography of the primary and secondary sympathetic trunks, but have not addressed the question whether the change in position is mediated by

a functional change in the neurons of the trunks (e.g. their synthesis of the BDNF receptor TrkB) or the result of differential changes in growth of surrounding structures.

In our studies of the extrinsic innervation in the abdomen and lesser pelvis (Kruepunga et al., 2020a; Kruepunga et al., 2020b), we identified neural crest-derived ganglionic cells by their intense staining properties and topography (cf. also (Lutz, 1968)). In these studies, we did not address the appearance and organisation of neural crest-derived cells that form the sympathetic trunks. In particular, we did not assess the putatively metameric organisation of the sympathetic trunks along their longitudinal axis, the polarity of their organisation along the radial axis, and their topographical relation to surrounding tissues. We addressed these questions by producing detailed reconstructions of the sympathetic trunks and their surroundings in nine embryos between 5 and 10 weeks of development. In addition, we quantified the distances between sympathetic trunks and surrounding landmarks to establish the time course and extent of the changes in topographic position of the developing sympathetic trunks.

2 | MATERIALS AND METHODS

2.1 | Embryos

This study was undertaken in accordance with the Dutch regulations for the proper use of human tissue for medical research purposes. Well-preserved anonymous human embryos and foetuses, donated for scientific research, of the historical collections of the Departments of Anatomy and Embryology, Leiden University Medical Centre (LUMC), the Amsterdam University Medical Centres, location Academic Medical Centre (AMC), Radboud University, Nijmegen, The Netherlands, and the University of Göttingen, Germany (Blechs Schmidt Collection; <https://doi.org/10.3249/ugoe-publ-2>) were studied (Table 1). In addition, digital images of carefully staged human embryos from the Carnegie collection (Washington D.C., USA) were included from the Digitally Reproduced Embryonic Morphology (DREM) project (<http://virtualhumanembryo.lsuhscc.edu>).

2.2 | Image acquisition, 3D reconstruction, and visualisation

Human embryos between 4.5 and 10 weeks post-fertilisation were investigated. The modified O’Rahilly criteria were used to define the Carnegie stage (CS) of development and post-fertilisation age [(O’Rahilly & Muller, 2010); Table 1]. Serial sections from the aforementioned collections were digitised with an Olympus BX51 or BX61 microscope and the Dotslide program (Olympus, Leiderdorp, The Netherlands) to provide high-resolution digital images. Serial sections of the Blechs Schmidt collection were digitised with a Zeiss Axio Scan.Z1 (Carl Zeiss Microscopy, Jena, Germany). All digital images were transformed into greyscale ‘JPEG’ format and imported into Amira (version 2019.4; FEI Visualization Sciences Group Europe,

TABLE 1 Metadata of human embryos and fetuses used in the study. The estimated post-fertilisation ages of the embryos are based on (O'Rahilly & Muller, 2010)

Stage	Days	Embryo	Fixation	Staining	Plane	Source
CS13	32	S836	HgCl ₂	CA	Transv	DREM
CS14-early	33	S2201	Formalin	H & A	Transv	AMC
CS14-mid	34	S5029	Formalin	H & A	Sagittal	AMC
CS14-mid	34	S168	Bouin's fix	H & E	Transv	LUMC
CS14-mid	34	1950-09-13	Bouin's fix	H & E	Sagittal	Göttingen
CS14-late	35	1958-12-22	Bouin's fix	H & E	Sagittal	Göttingen
CS14-late	35	1961-06-13	Bouin's fix	H & E	Transv	Göttingen
CS14-late	35	S6502	Souza's fix	H & E (or +Ag)	Transv	DREM
CS15-early	36	S721	Zenker's fix	H & E (or +Ag)	Transv	DREM
CS15-early	36	S79	Formalin	H & E	Transv	LUMC
CS15-early	36	1945-10-26	Bouin's fix	H & E	Transv	Göttingen
CS15-early	36	1957-10-31	Bouin's fix	H & E	Transv	Göttingen
CS15-late	37	S2213	Formalin	H & A	Transv	AMC
CS16	39	S5032	Formalin	H & A	Sagittal	AMC
CS16	39	S6517	Corrosive CH ₃ COOH	CA	Transv	DREM
CS16	39	S39	Formalin	H & E	Transv	LUMC
CS17	41	S6520	Corrosive CH ₃ COOH	CA (or +Ag)	Transv	DREM
CS18	44	S97	Bouin's fix	H & E	Transv	LUMC
CS18	44	S4430	Corrosive CH ₃ COOH	CA	Transv	DREM
CS19	46	S9325	Acetic formalin	Azan & Ag	Transv	DREM
CS20	49	S2025	Bouin's fix	H & A	Transv	AMC
CS20	49	S462	Formalin	CA	Transv	DREM
CS20	49	S34	Formalin & Bouin's fix	H & E	Sagittal	LUMC
CS21	51	S4090	Formalin	CA	Transv	DREM
CS22	53	S48	Formalin	H & E	Transv	LUMC
CS22	54	S983	Formalin	H & E	Transv	DREM
CS23	56	S4141	Formalin	H & A	Transv	AMC
CS23	56	S9226	Formalin	Azan	Transv	DREM
CS23	56	S88	Formalin & Bouin's fix	H or PAS or Azan	Sagittal	RadboudMC
9 weeks	63	S89	Formalin	H & E or Azan	Transv	LUMC
9.5 weeks	67	S57	Formalin	H & E	Transv	LUMC
10 weeks	70	S1507		H & A	Transv	AMC

The additions "early", "mid" and "late" are meant to indicate that, within these stages, the development of the gut and enteric nervous system of "late" embryos was more advanced than that of "early" embryos. The corresponding age was chosen from the range of developmental days attributed to that stage (O'Rahilly & Muller, 2010). CS14 is in particular noted for its remarkable number of developmental events. Abbreviations: AC, alum cochineal (i.e., carmine); AMC, Academic Medical Centre; CS, Carnegie stage; DREM, Carnegie collection from the Digitally Reproduced Embryonic Morphology project; Göttingen, Department of Anatomy and Embryology, Göttingen; H&A, haematoxylin and azophloxine; H&E haematoxylin and eosin; LUMC, Leiden University Medical Centre; PAS, periodic acid-Schiff stain; RadboudMC: Radboud Medical Centre.

Merignac Cedex, France). The imported images were aligned automatically with the least-squares function and then manually corrected for their embryonic curvature with the aid of photographs and magnetic resonance images (MRI) of the same stages of human embryos (Pooh et al., 2011). The criteria used to identify agglomerates of scattered neural crest cells were cell staining properties (intensely basophilic), cell density, and cell distribution. Developing nerve fibres were characterised by their intensely acidophilic staining property and filamentous distribution. These criteria allowed for

sensitive and accurate segmentation throughout early development (Figure S1). In later stages, the borders of the neural agglomerates and their connecting nerve fibres became more distinct. Based on these criteria structures of interest were identified and segmented manually to generate three-dimensional images with the Amira program. To exclude the distracting noise from section processing and stacking in the Amira output, Amira polygon meshes were exported via 'vrml export' to Cinema 4D (version R21; MAXON Computer GmbH, Friedrichsdorf, Germany) and remodelled using the Amira

model as a template. Synchronous visualisation of the Amira template and the remodelled Cinema4D model in Cinema 4D was used to validate the accuracy of the Cinema4D models (Figure S2). The Cinema4D models were transferred via 'wrl export' to Adobe Acrobat version 9 (<http://www.adobe.com>) to generate interactive 3D Portable Device Format (PDF) files, which are a user-friendly format for 3D visualisation (Figures S1 and S4). We mostly refer in the text to the Figures to relate histology to developing structures, but encourage the reader to simultaneously inspect the interactive PDFs, because their rotational options ("live" images) allow a much better understanding of the complex local topography than the "still" pictures in the images.

2.3 | Measurements

All morphometric analyses were performed in Amira. The data were subsequently analysed in Microsoft Excel (Microsoft Corporation, Washington, USA). Analyses included topographic position of sympathetic ganglionic cells and nerve fibres, and distances between four landmarks. These landmarks were the middle of the floor plate of the spinal cord, the notochord, the centres of the sympathetic ganglia, and the middle of the dorsal side of the aorta. The segmental positions were determined perpendicular to the embryonic axis (notochord). The first cervical level was defined as the first segment in this study.

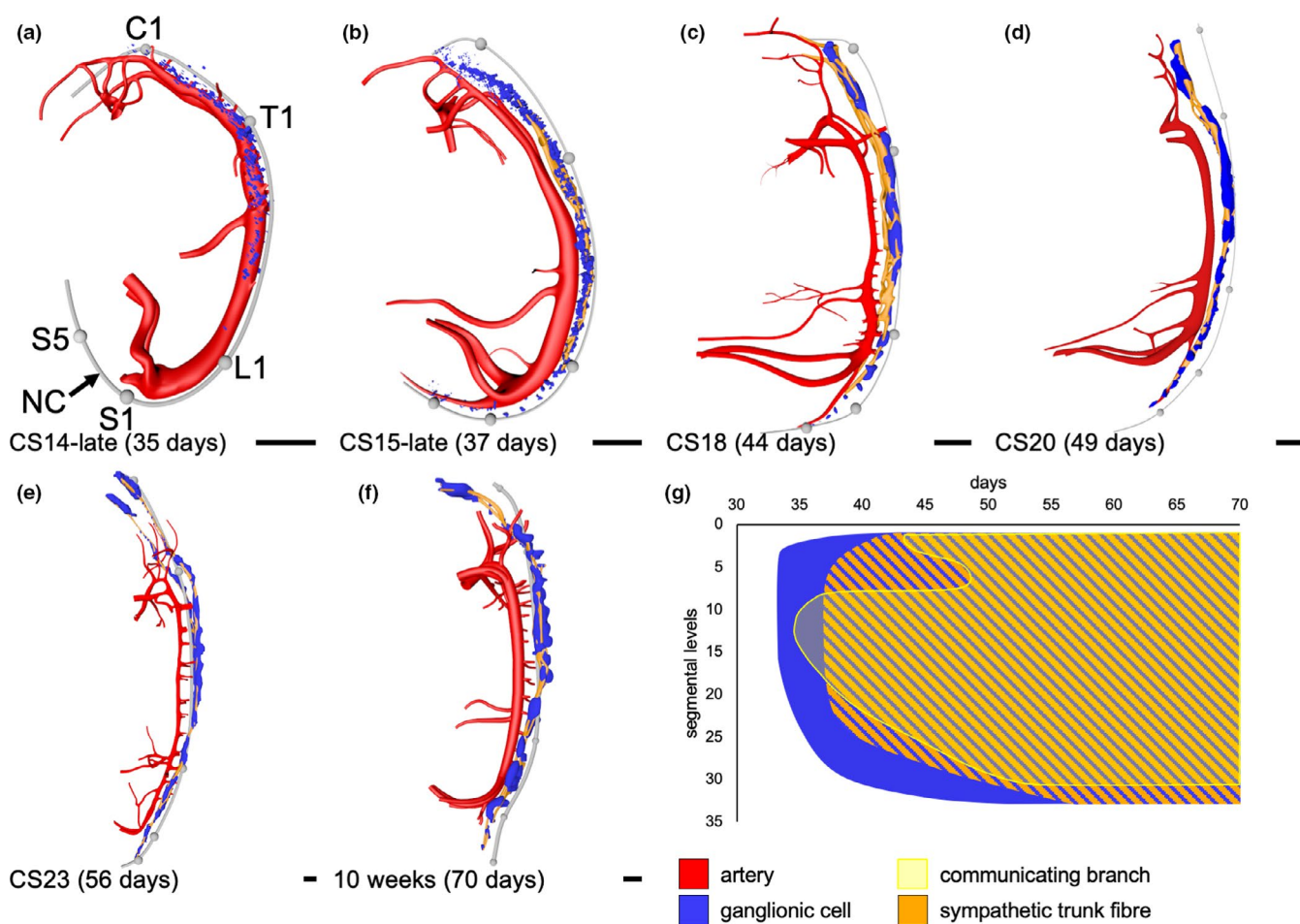


FIGURE 1 Spatiotemporal distribution of the ganglionic cells and the nerve fibres of the sympathetic trunks. Panels (a–f) show left-sided views of the topographic distribution of the sympathetic trunks along the aorta and notochord (NC; grey). The spheres on the notochord represent the first cervical (C1), first thoracic (T1), first lumbar (L1), first sacral (S1), and fifth sacral (S5) segmental levels. Segmental levels are determined by counting the spinal ganglia. Spinal ganglia are not shown in the images, but are included in the reconstructions. Panel (g) shows the spatiotemporal distribution of ganglionic cells (blue), sympathetic trunk fibres (orange), and communicating branches (transparent yellow). At CS14-late (~35 days; panel (a)) dispersed ganglionic cells (blue) are present between C3 and T8. Subsequently (CS15-late, ~37 days; panel (b)), ganglionic cells extend cranially to reach C1 and caudally to reach S1 levels. Concomitantly, nerve fibres (yellow) have formed between C4 and L1. One week later (CS18, ~44 days; panel (c)), ganglionic cells have extended caudally to S5, whereas nerve fibres reach S5 (panel (e)) only 2 weeks later. These data are summarised in panel (g). Bar = 500 μ m. Note that the sympathetic trunks of the coccygeal region are not shown in panels (e) and (f), because the pertinent sections were not available

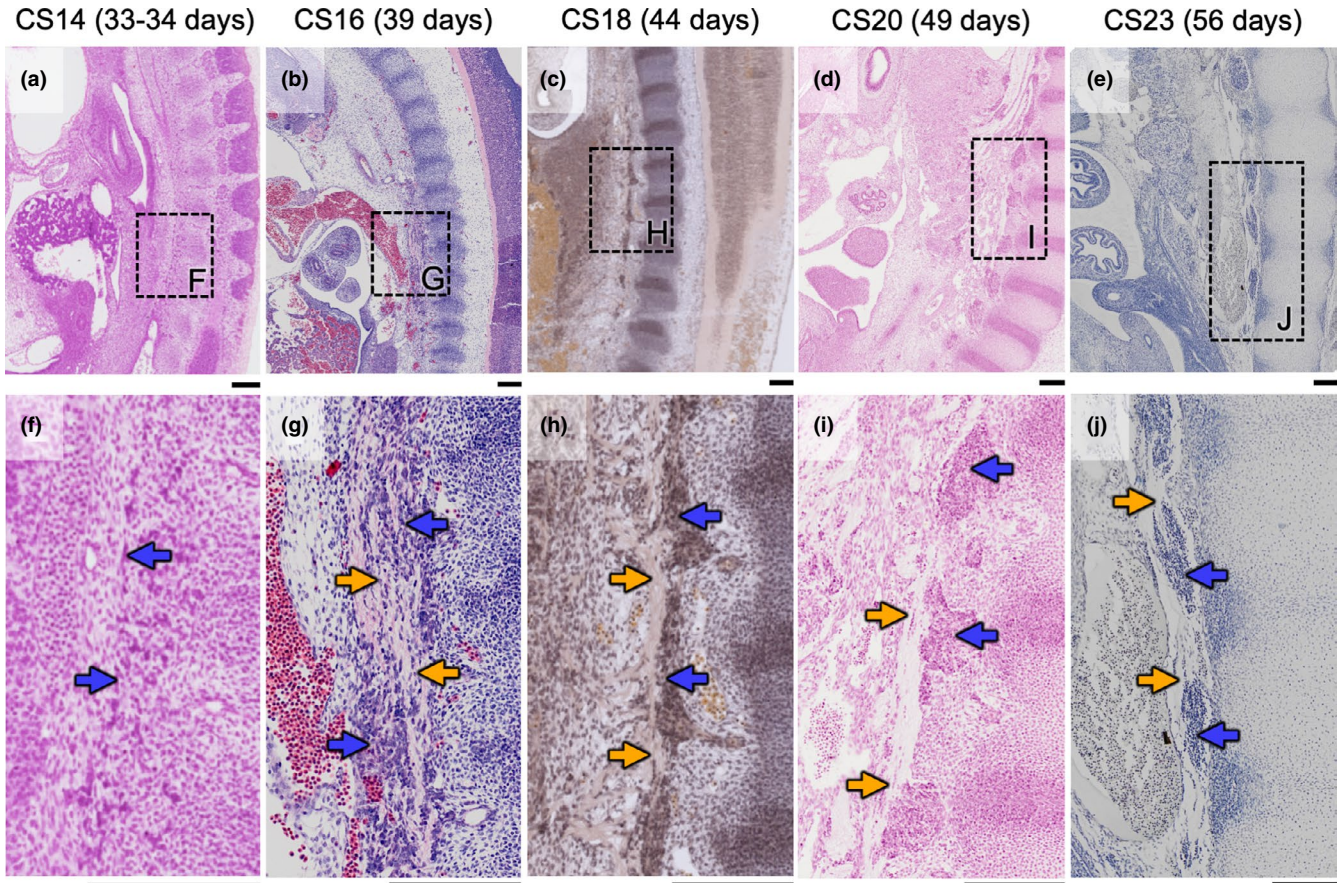


FIGURE 2 Organisation of the ganglionic cells and the nerve fibres in the sympathetic trunks. Panels (a–e) are overviews of sagittal sections that show the locations of the magnified areas (rectangles) in panels (f–j). The magnifications show the distribution of ganglionic cells (blue arrows) and nerve fibres (yellow arrows) forming the sympathetic trunk. At CS14 (33–34 days; panel (f)) the sympathetic trunks consist of diffuse ganglionic cells only (blue arrows). Two stages later (CS16; ~39 days; panel (g)) nerve fibres (yellow arrows) become identifiable. At this stage, ganglionic cells and nerve fibres are distributed randomly within the sympathetic trunks (panel (g)). At CS18 (~44 days; panel (h)), the sympathetic trunks begin to assume a pearls-on-a-string appearance, while this configuration is clearly established at CS20 (~49 days). The pearls are represented by the segmental aggregations of ganglionic cells into ganglia that mainly locate to the dorsal side of the sympathetic trunks, whereas the strings are nerve fibres that are exclusively found on the ventral side of the trunks. Note that the ganglia match with the vertebrae in the cranial portion of panel (d), but with the intervertebral disk caudally. The sympathetic trunks retain the pearls-on-a-string appearance at CS23 (~56 days; panel (j)), but ganglia now occupy a more central position in the trunks. Bars =200 μ m

3 | RESULTS

3.1 | Formation of the sympathetic trunks

The sympathetic trunks form from scattered, intensely staining neural crest cell-derived ganglionic cells (Furlan & Adameyko, 2018; Kuntz, 1920). No cells with these characteristics are found near the dorsal aortae of a well-preserved CS13 embryo. Such cells do, however, appear laterally to the dorsal aorta in the lower cervical and upper thoracic levels at CS14-early (~33 days of development). In the next few days (CS14-late; ~35 days), the number of ganglionic cells increases greatly (Figure 1a). In the lower cervical and upper thoracic region these scattered ganglionic cells form longitudinal columns between the entrance of a spinal nerve into the dermomyotome laterally and the aorta medially (Figure 2a and f), while others are found more ventrally to the pre-aortic region (not shown, but described

at length in our earlier studies (Kruepunga et al., 2020a; Kruepunga et al., 2020b). The sympathetic trunk at CS14 consists of ganglionic cells only (blue dots in Figure 1a and blue arrows in Figure 2f), although nerve fibres from spinal nerves are already extending medially towards the forming columns of ganglionic cells to form the so-called “communicating branches” (cf. Figure 2 in (Kruepunga et al., 2020a)). These nerve fibres reach and become incorporated in the sympathetic trunk between CS15-late and CS16 (37-39 days). The sympathetic trunks at this stage are, therefore, composed of randomly distributed ganglionic cells intermingled between nerve fibres (blue dots and orange cords in Figure 1b; blue and orange arrows, respectively, in Figure 2g). From CS18 onwards (44 days), ganglionic cells manifest themselves as irregular agglomerates (ganglia) along a continuous cord of nerve fibres.

Simultaneously with the patterning of sympathetic trunks along the craniocaudal axis, ganglionic cells and nerve fibres separate

along the dorsoventral axis. Compared to the random distribution of ganglionic cells and nerve fibres in the forming trunks of CS15-16 embryos (Figures 1b and 2g), the ganglionic cells have aggregated on the dorsal side of the sympathetic trunks, whereas the nerve fibres concentrate more ventrally from CS18 onward (blue dots and orange cords in Figure 1c-f; blue and orange arrows, respectively in Figure 2h-j). This configuration is often described as ganglionic cells becoming organised in a pearl-necklace-like fashion along the nerve fibres, but it should be noted that both size and distribution of the pearls are markedly heterogeneous (Figures 1 and 2).

3.2 | Spatiotemporal appearance of the components of the sympathetic trunks

Sympathetic trunks consisting of ganglionic cells become identifiable at CS14-early (~33 days). At CS14-late (~35 days), these ganglionic cells are found between cervical somite 3 and thoracic somite 8 (C3-T8), that is, across ~15 segments. Two days later (CS15-late) ganglionic cells have reached C1 cranially. Caudally, the ganglionic cells reach L2 at CS15-early (~36 days), S1 at CS15-late (~37 days), S5 at CS16 (~39 days) and the coccygeal region at CS22 (~53 days; Figure 1). The rate of caudal extension of the sympathetic cells, therefore, gradually declines from ~6 segments per day at the end of CS14, via four segments per day during CS15, to 2 segments during CS16, and much slower in the caudal-most part (blue surface in Figure 1g). Nerve fibres are first seen in the sympathetic trunk at CS15-late (37 days) between C4 and L1 (Figure 1b; vertical leg of hatched orange surface in Figure 1g), which is ~2 days after the ganglionic cells have made their appearance. The nerve fibres have arrived at C1 at CS17 (41 days),

so extend ~1 segment per day. The ganglionic cells, therefore, reach the cranial end of the vertebral column ~4 days ahead of the nerve fibres (Figure 3). Accordingly, they are found migrating along the future internal carotid arteries before nerve fibres are present (Figure 3b). Caudally, the ganglionic cells reach L5 at CS18 (44 days), S3 at CS20 (49 days) and the coccygeal region around CS22-CS23 (53-56 days; Figure 4), which represents a linear extension of ~0.6 segment per day (oblique lower leg of hatched orange surface in Figure 1g). The nerve fibres of the sympathetic trunk extend, therefore, much slower along the body axis than the ganglionic cells, but at a constant pace.

3.3 | Regional differences in the configuration of the sympathetic trunks

As the ganglionic cells and the nerve fibres become organised in a pearl-necklace-like fashion between CS15-late and CS18 (37-44 days), the ganglia remain markedly heterogeneous both with respect to size and distribution (Figures 1 and 3). The most cranial, or superior cervical ganglion (SCG) of the sympathetic trunk forms, for example, far away from, and is larger than the adjacent inferior cervical (stellate) ganglion at the thoracic inlet. Both ganglia are further apart than more caudal ganglia (Figures 1 and 3; (Rubin, 1985)). It should be noted, however, that a separate middle cervical ganglion was not observed. The distance between the superior and inferior cervical ganglia increases with development, in particular after CS18 (Figures 1 and 3), which correlates temporally with the formation of the neck. At CS22 (~53 days) the sympathetic trunks in the lumbar and sacral region consists of the standard two columns of ganglionic cells and nerve fibres lateral to the median sacral artery and ventral

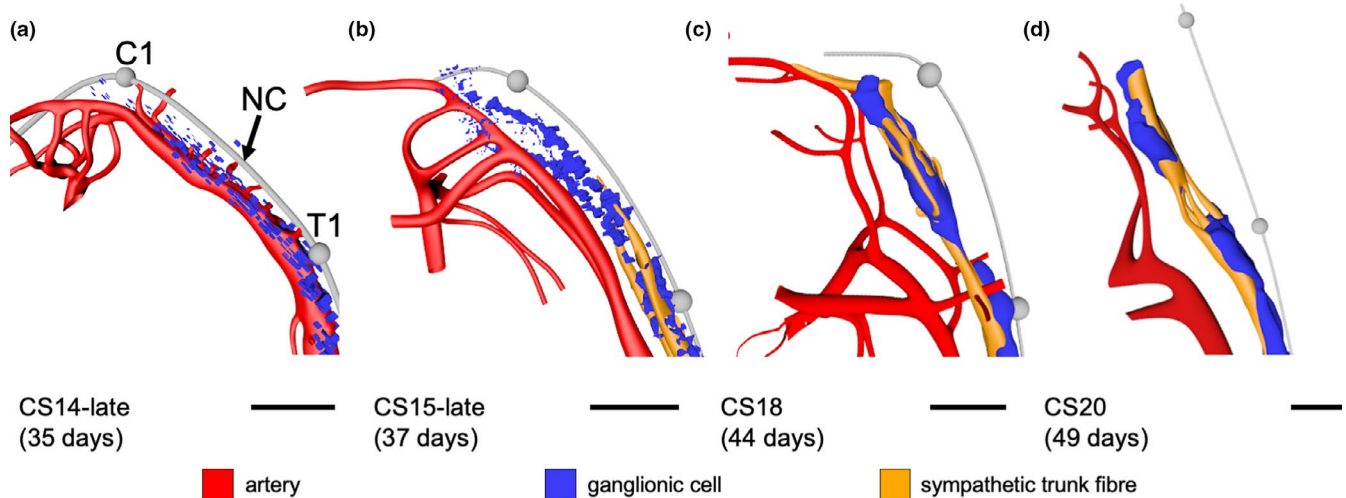


FIGURE 3 3Cranial expansion of the sympathetic trunks. Panels (a-d) show left-sided views of the cranial end of the sympathetic trunks between 5 and 7 weeks of development. At 5 weeks the main group of ganglionic cells (blue) have reached C3 cranially, although a few ganglionic cells have already passed (C1). Ganglionic cells accumulate cranially in the next 3 days (panel (b)). In contrast nerve fibres (yellow) emerge later and extend more slowly in cranial direction than the ganglionic cells. They arrive at C4 at 37 days and need another week to reach C1 (panel (c)). Meanwhile, ganglionic cells have arrived at the base of the skull. Note that nerve fibres in panel (d) were reconstructed only up to level C1. Bar =500 μ m

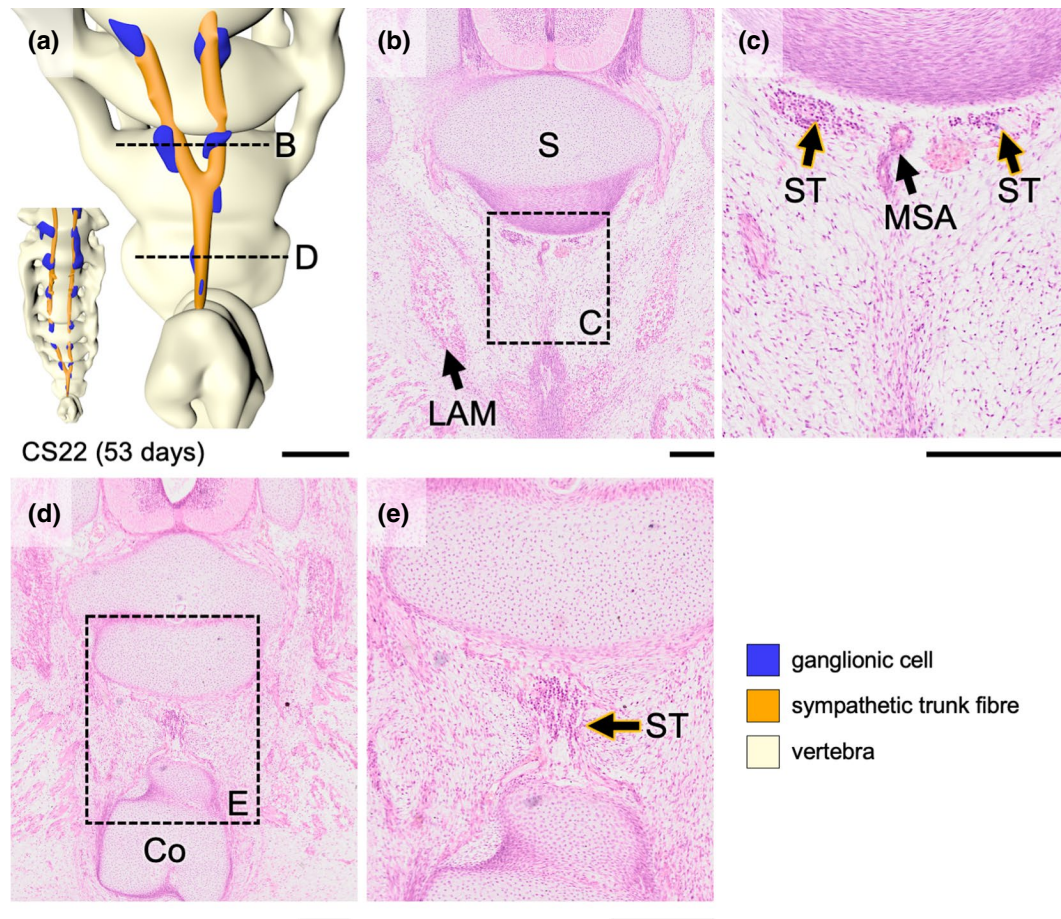


FIGURE 4 Caudal portion of the sympathetic trunks. Panel (a) shows a ventral view of the caudal part of the sympathetic trunks with sacrum and coccyx at CS22. Panels (b) and (d) show transverse histological sections of the sympathetic trunks at the levels indicated by dashed lines in panel (a), whereas magnifications of the boxed areas in panels (b) and (d) are shown in panels (c) and (e). At CS22 the sympathetic trunks (ST) in the sacral region (panel (c)) consist of two columns of ganglionic cells and nerve fibres lateral to the median sacral artery (MSA). Caudally, both sympathetic trunks (ST in panel (e)) converge into a single trunk with ganglia (panel (a)) in front of the coccygeal vertebrae (Co). The medial sacral artery is not present at this level. Bar A = 500 μm and bars (b–e) = 200 μm

to the vertebral column (Figure 4a–c), but both trunks converge into a single column of ganglionic cells and nerve fibres in front of the coccygeal vertebrae. Usually, a single unpaired precoccygeal ganglion is described as the ganglion impar (Paterson, 1890), but we observed two small unpaired ganglionic agglomerates (Figure 4a, d and e). The medial sacral artery is not present at this level.

3.4 | Nervous connections of the sympathetic trunks

Each sympathetic trunk forms one cranial and two main segmental nervous connections. The cranial part of the sympathetic trunk contacts the vagus nerve at CS15-late. We observed ganglionic cells (blue arrows in Figure 5b) along the internal carotid artery (ICA) between the sympathetic trunk (ST; black arrow) and the nodose ganglion (white-lined, olive-coloured dotted contour) of the vagus nerve (orange dotted contour; Figure 5b and c). Like the communicating branches, we do not know the direction of nerve signalling. We did not follow the migratory

route of ganglionic cells along the ICA in the older embryos. Earlier studies have shown that ganglionic cells that migrate in the wall of the ICA populate the cranial ganglia (Andres & Kautzky, 1955; Streeter, 1912).

The first connection consists of segmentally organised nerve connections between the spinal nerves and sympathetic trunks, which are known as the communicating branches (golden arrowheads in Figure 5e and f; (Kruepunga et al., 2020a)). The first communicating branches are tiny nerve fibres between vertebral levels T3–T4 at CS14-late [35 days; Figure 2 in (Kruepunga et al., 2020a)]. Between CS15 and CS18 (37–44 days) communicating branches are present between C8 and L2 (Figure 1g). Interestingly, communicating branches, which join the developing superior cervical ganglion, are also present at segments C1 and C2, but not between C3 and C7 until CS18-late and older embryos. At CS20 (~49 days), such communicating branches are present from level C1 cranially to S1 caudally. Segmental level S4 is reached at CS22 (53 days) (transparent yellow area in Figure 1g, Figure S3 and S4). Communicating branches, therefore, reach the sympathetic trunks at the same time as, or shortly after nerve fibres appear in the trunks themselves.

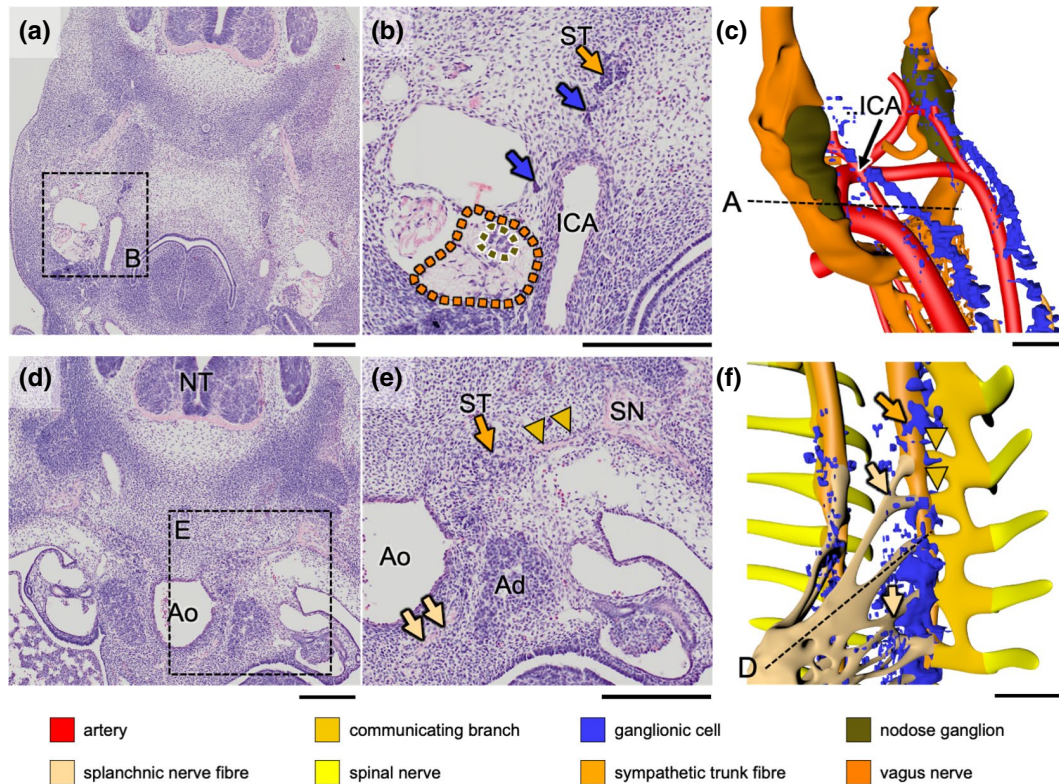


FIGURE 5 Nervous connections of the sympathetic trunks. Panels (a, b, d and e) show transverse histological sections of the sympathetic trunks and their connections at the level of the nodose ganglion of the vagus (a–c) and at the level of the celiac plexus (d–f), with the plane of the sections indicated by the dashed lines in panels (c) and (f). In the upper row, ganglionic cells (blue arrows in panel (b)) migrate along the internal carotid artery (ICA) towards the nodose ganglion (olive colour code in panels (b) and (c), with white lining in panel (b)) that is itself embedded in vagus nerve fibres (darker orange colour code in panels (b) and (c), with black lining in panel (b)). In the lower row, a column of the sympathetic trunk (ST, black) appears to function as a hub: spinal nerves (SN) extend medially towards the sympathetic trunk as communicating branches (yellow arrowheads in panels (e) and (f)) or pass the sympathetic trunk and continue ventrally as a splanchnic nerve (beige arrows in panels (e) and (f)). Bars = 200 μ m

The staining of the embryos does not allow differentiation between white and grey communicating branches.

Splanchnic nerves pass through, but do not synapse in the ganglia of the sympathetic trunk. In Figure 5 (beige arrows in panels (e) and (f)) they can be seen between the sympathetic trunk and the pre-aortic coeliac plexus. The splanchnic nerves start to extend ventrally as scattered ganglionic cells at CS15-late (37 days), but have reached the pre-aortic ganglia at this stage only at the level of the coeliac trunk. We have described the spatiotemporal development of the splanchnic nerves in our studies on the autonomic innervation of the abdominal and pelvic intestines (Kruepunga et al., 2020a; Kruepunga et al., 2020b).

3.5 | Change in topography of the sympathetic trunks

It is well established that the sympathetic trunks change their topographical position relative to the vertebral column with ongoing development (Gibbins, 1994; Kasemeier-Kulesa et al., 2015; Kuntz, 1920). The cited studies use the change in position of the trunks from lateral (“para-aortic”) to dorsolateral (prevertebral or paravertebral) relative to the aorta as a criterion to mark the transition from primary

to secondary sympathetic trunks. At CS14-late (35 days), the scattered ganglionic cells are considered to occupy a para-aortic position (Figure 6a). At CS15-late (37 days), the sympathetic trunks in the cervical and upper thoracic region have acquired a prevertebral position between the aorta ventrally and the vertebral column dorsally. The developing trunks in the lumbar and sacral region still occupy a para-aortic position. The lower thoracic and lumbar sympathetic trunks acquire a prevertebral position at CS18 (Figure 6c). Between CS18 and CS23 (44–56 days), only the position of the thoracic sympathetic trunk continues to move further dorsally to a paravertebral position (Figure 6c–e). The columns of the sympathetic trunk in the sacral region remain positioned lateral to the median sacral artery (morphologically the caudal continuation of the dorsal aorta) and in front of the sacrum between CS23 and 10 weeks. Their position is, therefore, considered as both para-aortic and prevertebral (Figure S5).

To quantify the change in the position of the sympathetic trunks relative to the vertebral bodies, we measured four distances between landmarks surrounding the sympathetic trunks, including the middle of the floor plate of the spinal cord, the notochord (the vertebral column becomes identifiable only at CS15-late), the centres of the sympathetic trunks, and the middle of the dorsal aortic wall. All distances were measured at 4 vertebral levels: T2, T7, L1, and S1

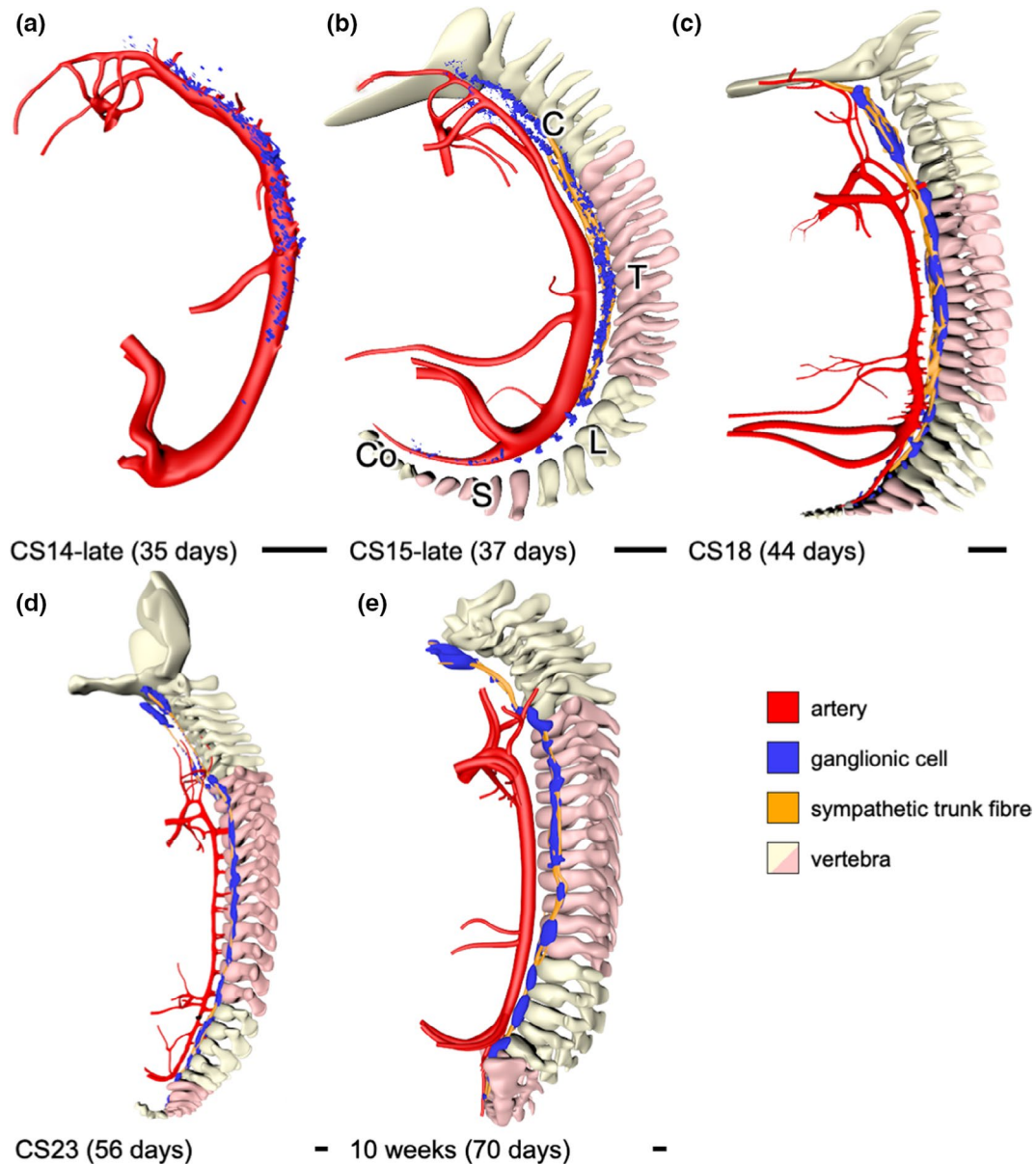


FIGURE 6 Changes in the topographical position of the sympathetic trunks. Panels (a–e) show left-sided views of the topography of the sympathetic trunks relative to the aorta and vertebral column. At CS14-late (~35 days) and before a vertebral column can be recognised, the ganglionic cells (blue) at the cervical (C) and thoracic (T) levels occupy a para-aortic position. At CS15, the mesenchymal condensations of the vertebrae have appeared (panel (b); (Mekonen et al., 2015)). At this stage, sympathetic ganglionic cells and nerve fibres at the cervical, thoracic, and lumbar levels have acquired a position between aorta and vertebral column (prevertebral). Only the sympathetic trunks in the thoracic region shift further dorsally to acquire a paravertebral position at CS23 and an even more distinct paravertebral position at 10 weeks (upper pink region in panels (c–e)). In contrast, the sympathetic trunks in the sacral region retain their para-aortic and simultaneously prevertebral position (lower pink region in panel (c–e); cf. black-lined rectangles in Figure 8). Bars = 500 μ m

(Figure 7a). The distances between the floor plate of the spinal cord and the notochord (line AB, Figure 7b) increase at a similar rate at all measured vertebral levels. The distance increases between CS16 and CS18, plateaus temporarily between CS18 and CS23, to increase again thereafter. The line connecting the notochord and the dorsoventral position of the centres of the sympathetic trunks (line BE, Figure 7c) hardly changes until CS21, after which the thoracic lines decline abruptly, in agreement with the change in position of the sympathetic trunks to paravertebral. At the lumbar and sacral

levels, however, this distance hardly changes until CS23, after which it increases between weeks 9 and 10. The data in panels B and C indicate overall vertebral growth at the lumbar and sacral levels without change in position of the trunks. The distance between the left and right columns of the sympathetic trunk (line CC, Figure 7d) and that between the sympathetic trunks and the dorsal aortic wall (line CD, Figure 7e) change with a similar pattern: steady growth between CS15 and 9 weeks, which is most pronounced in the upper thoracic region and slowest in the sacral region, with T7 and L1 again taking

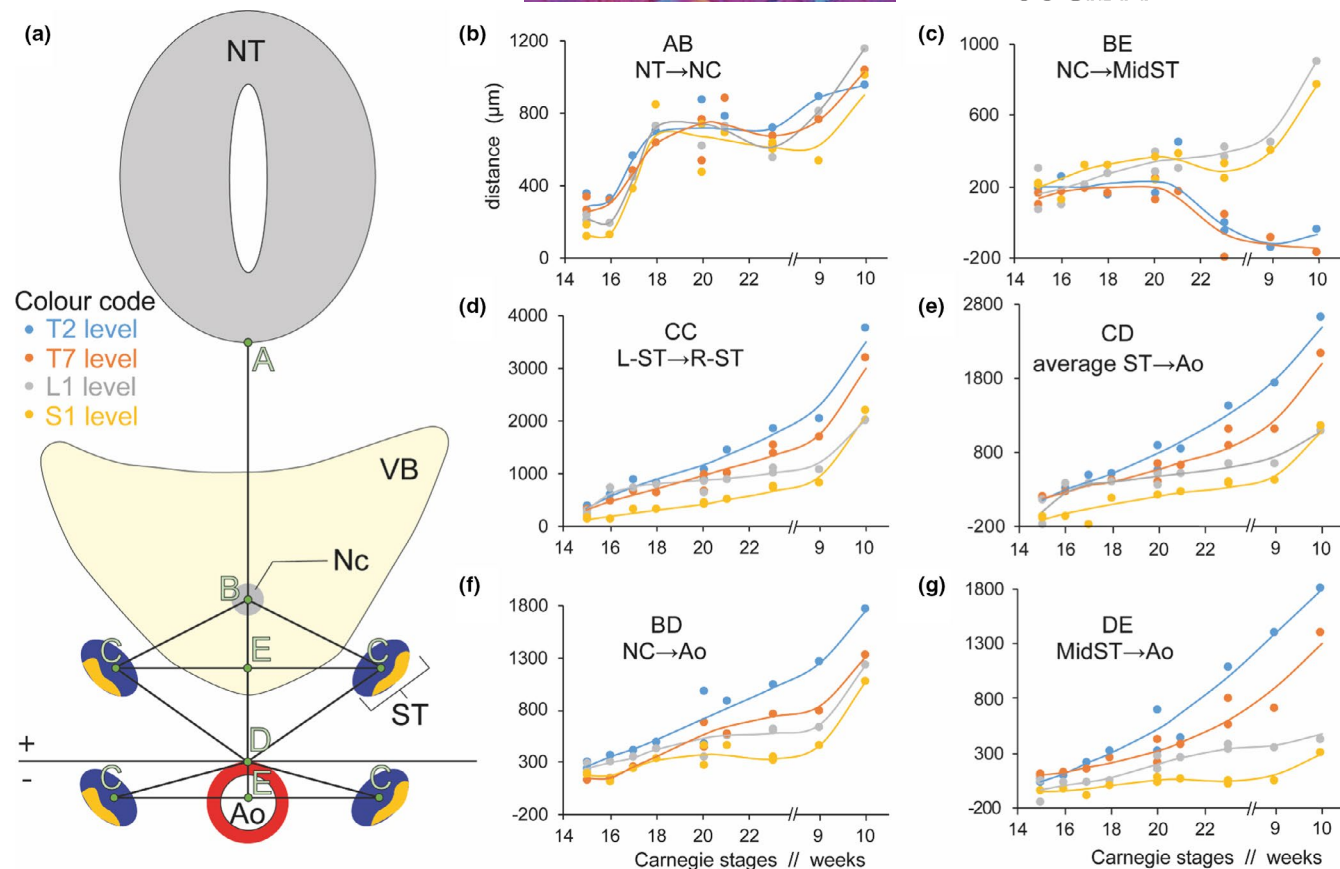


FIGURE 7 Changes in topographical position of the sympathetic trunks along the vertebral column. Panel (a) shows the landmarks and distances measured or calculated. Panels (b–g) show the distances indicated by landmarks in panel (a) at five different vertebral levels: T2 (blue lines), T7 (orange lines), L1 (grey lines) and S1 (yellow lines). Note that distances acquire negative values when the sympathetic trunks (landmark C) pass the horizontal line through landmark D, which happens when landmark C lies lateral rather than dorsolateral to the aorta. The distances between the floor plate of the spinal cord and the notochord (line AB, panel (b)) change in a comparable fashion at all measured vertebral levels: a rise between CS16 and CS18, a plateau between CS18 and CS23, and then again a rise. The distance between the notochord and the middle of the bilateral sympathetic trunks (line BE, panel (c)) shows little change until CS21, after which the thoracic lines decline abruptly, due to a dorsal relocation of the sympathetic trunks relative to the vertebrae. The lumbar and sacral lines, instead, show little change in position until they rapidly increase in length between weeks 9 and 10. The distance between both sympathetic trunks (line CC, panel (d)) and average distances (left and right) between the sympathetic trunks and aorta (line CD, panel (e)) change according to a similar pattern: steady growth between CS15 and 9 weeks, which is faster cranially than caudally, followed by an acceleration between 9 and 10 weeks. The distance between the aorta and the middle of the bilateral sympathetic trunks (line BD, panel (f)) or the notochord (line DE, panel (g)) increases with different characteristics along the vertebral column: at the thoracic level there is a smooth increase in distance between CS15 and 9 weeks, after which growth accelerates, but more caudally, the growth rate increasingly resembles that seen in panel (b), indicating that the vertebrae grow more homogeneously in all directions at the lumbar and sacral levels. Abbreviation: VB; vertebral body

intermediate positions. At all vertebral levels, growth accelerates in the 10th week.

The distance between the aorta and the notochord (line BD, Figure 7f) or the aorta and the middle of the bilateral sympathetic trunks (line DE, Figure 7g) increases with different characteristics along the vertebral column: at the thoracic level there is a smooth increase in distance between CS15 and 9 weeks, after which growth accelerates; more caudally, the growth rate increasingly resembles that seen in Figure 7b, further supporting the conclusion from panels (b) and (c) that the caudal vertebrae expand more homogeneously in all directions. In aggregate, these findings show that differential growth causes the sympathetic trunks in the thoracic region to change position in dorsolateral direction relative to the aorta, whereas the sacral

region experiences more homogeneous growth so that the original position of the sympathetic trunks is virtually retained. The data further show that only the thoracic sympathetic trunks assume a paravertebral position, and that this change in position occurs between CS20 and CS23, that is, during the 8th week of development. The outcome of these measurements is presented schematically in Figure 8.

4 | DISCUSSION

The sympathetic trunk is part of the sympatho-adrenal lineage. Descriptions and illustrations of the migratory pathway and developmental appearance of the cells of the sympathetic trunks are

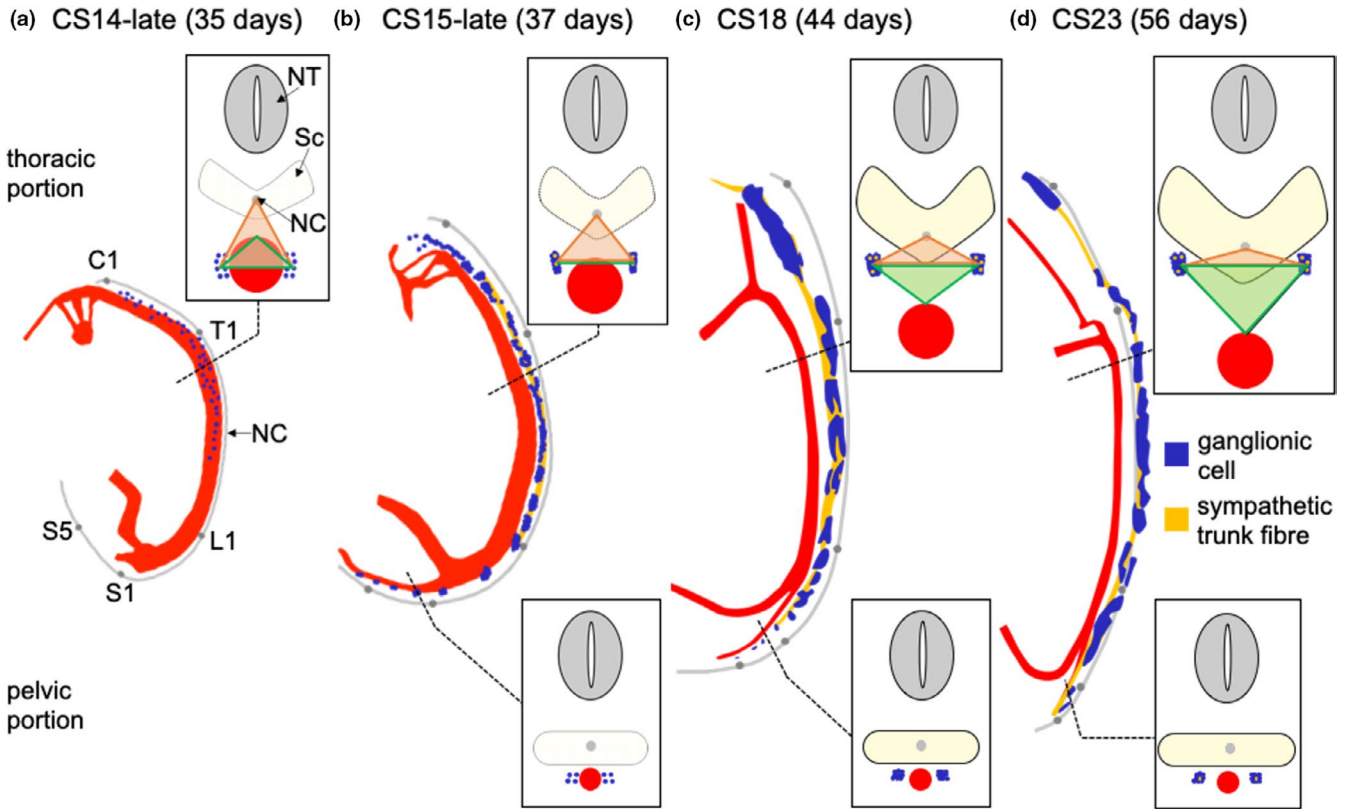


FIGURE 8 Regional patterns in the changing topography of the sympathetic trunks. Panels (a–d) show the topography of developing sympathetic trunks between 5 and 8 weeks of development. The dotted lines indicate segmental level T1 and S1, and the boxed subpanels the corresponding schematic sections. The upper row of boxes shows the thoracic cross sections and the lower row the sacral ones. To demonstrate the topographical change in sympathetic trunks, two triangles were drawn. Both triangles share their bases in the centres of both sympathetic trunks. The ventral triangles (green) have their apices on the dorsal wall of the aorta, whereas the dorsal triangles (orange) have them on the notochord. The scheme shows that the sympathetic trunks change their position from para-aortic at 5 weeks of development to paravertebral at 8 weeks of development in the thorax, but that no change in position occurs at the sacral level. Figure 7 demonstrates that the cranio-caudal difference in position occurs in the 8th week of development between vertebrae T7 and L1

often limited to the thoracic level, where the lineage is first identifiable and where the developing adrenal medulla is also present (Chan et al., 2018; Furlan et al., 2017; Saito & Takahashi, 2015). In the present study, we have studied the appearance of ganglionic cells and nerve fibres in the sympathetic trunks separately, using their morphological characteristics in the stained sections. We observed that the sympathetic trunks become recognisable as a chain of ganglionic cells in the cervical and upper thoracic levels of CS14 embryos. Although the time of first appearance of the sympathetic trunks was similar in our study and earlier reports (Kuntz, 1920; Woźniak et al., 2009), we localised the segmental level at which these early trunks formed as the lower cervical and upper thoracic levels, whereas Woźniak identified the mid-thoracic levels (Woźniak et al., 2009), and Kuntz the lower thoracic and upper lumbar levels (Kuntz, 1920). We based our assessment of the segmental levels on whole-body reconstructions of embryos and counting of the spinal ganglia in these reconstructions, whereas the method to assess segmental levels was not reported in the earlier studies (Kuntz, 1920; Woźniak et al., 2009). The elongation of the trunks is fast in cranial direction,

but proceeds at a progressively slower pace in caudal direction to reach the coccygeal level only at CS22–23. The nerve fibres of the trunks and the communicating branches with the spinal nerves were established during CS15 and CS16. The typical pearls-on-a-string appearance of ganglia and nerve fibres became established during CS18, with the beads being markedly heterogenous in size, and irregular in appearance and distribution. Coincident with the formation of the neck, the cranial part of the trunks with the superior cervical ganglion became markedly longer after CS18. Furthermore, the trunks assumed a markedly more dorsolateral (prevertebral) position cranially than caudally, which was found to be due to differential growth of the surrounding mesenchyme (Figure 8).

4.1 | Spatiotemporal changes in the developing sympathetic trunks

In standard textbooks, the ganglia of the sympathetic trunks are very homogeneous in size and distribution along the sympathetic

trunks. This representation classically underlies the elegant pearls-and-necklace metaphor. The metaphor is also misleading, however, since we show that the pearls are markedly irregular in shape and distribution along the necklace (Figure 8). The formation of the sympathetic trunk can be divided into three main steps. When the neural crest cells move ventrally to their para-aortic position, they pass in a metameric fashion through the cranial half of somites, only to re-aggregate again into a continuous chain of ganglionic cells lateral to the aorta [Figure 2; (Gammill & Roffers-Agarwal, 2010; Kulesa et al., 2009)]. Next, the sympathetic trunks extend non-metamerically along the entire post-cranial length of the embryo and produce nerve fibres (orange colour code in Figure 1). Trunk extension and production of nerve fibres starts in the lower cervical and thoracic regions, and extends from there in cranial and caudal directions, with extension and fibre formation progressing faster cranially than caudally (Figure 1). The relatively slow neuronal development in the pelvic region was also observed for other extrinsic nerve fibres that form in this region (Kruepunga et al., 2020a). Segmentation of the trunks into agglomerates of ganglionic cells and areas almost devoid of ganglionic cells is the final step in sympathetic trunk formation. This distribution of the sympathetic ganglia becomes more-or-less periodical in appearance at 7 weeks of development, but does not correlate well with segments or vertebrae (Figure 1d; cf. (Fernholm, 1971) for mouse embryos). The re-segmentation is also markedly irregular, with larger, seemingly fused ganglia and smaller, so-called intermediate ganglia (Figure 2i; Groen et al., 1987; Wrete, 1959)). Re-segmentation is reportedly dependent on somitic segmentation (Gammill & Roffers-Agarwal, 2010; Goldstein & Kalcheim, 1991), but may also be dependent on local factors (Kasemeier-Kulesa et al., 2005), and perhaps be related to the segmental distribution of preganglionic sympathetic nerves or communicating branches (Kasemeier-Kulesa et al., 2015).

4.2 | Differential growth as cause of the succession of the primary and secondary sympathetic trunks

The succession of the primary by the secondary sympathetic trunks is mainly based on a change in topographical position. The para-aortic "primary" sympathetic trunks are the early craniocaudal strands of neural crest cells (Huber, 2006; Kameda, 2014), while the "secondary" or definitive sympathetic trunks occupy a more dorsolateral and, therefore, pre- or even paravertebral position (Gibbins, 1994; Kuntz, 1920). The ganglionic cells of the primary trunks still divide, but express an aminergic phenotype (Cocharde et al., 1979; Rothman et al., 1978), suggesting that they already represent an early phase of differentiation. More recently, it was reported that the ganglionic cells of the primary sympathetic trunk acquired the paravertebral position of the secondary trunk by backtracking along their original migratory pathway due to chemotactic attraction by preganglionic axons exiting the spinal cord (Kasemeier-Kulesa et al., 2015). In the present study, we showed that regional differences in growth rate

also contribute to the change in position of the sympathetic trunks. Obviously, both processes are not mutually exclusive.

While our observations suggest a role for vertebral growth, we wondered why the observed changes were limited to the thoracic region. In the 8th and 9th weeks, the midthoracic vertebrae stand out in being more advanced in the development of their neural arches than more cranial or caudal vertebrae (Mekonen et al., 2017). Interestingly, midthoracic development is also more advanced on the ventral side of the vertebrae. Between CS17 and CS19, a subcoelomic mesenchymal body of considerable size develops between the vertebral bodies and ribs dorsally, and the parietal pleura ventrally, only to rapidly disappear during CS20 and CS21 to allow expansion of the pleural cavity (Frick, 1949; Salzer, 1960). The removal of the subcoelomic mesenchyme by apoptosis also begins in the midthoracic region and does not seem to be dependent on the presence of lungs (Norden et al., 2010; Salzer, 1960). Furthermore, the rib cage rapidly widens and deepens starting at CS20, in particular in the midthoracic region (Mekonen et al., 2015; Okuno et al., 2019). These observations show that the midthoracic region is a leading centre of the development of the vertebral column and suggest that differential growth along the vertebral column is an important determinant of the dorsoventral position of the sympathetic trunk on the vertebral bodies. This timeline contrasts with the growth patterns of the lumbar and especially the sacral area, which only begin to accelerate in the 10th week of development. This finding is in line with our earlier observation that growth and closure of the neural arch of the sacral vertebrae is delayed relative to more cranial vertebrae, but resumes between 9 and 10 weeks of development (Mekonen et al., 2017).

The cranio-caudal difference in the position of the sympathetic trunks has thus far attracted relatively little attention due to the focus of studies on the thoracic region (see our Introduction). To address this issue, we show trunks and aorta schematically in Figure 8, which is based on the measurements shown in Figure 7. The lateral views of the sympathetic trunks and dorsal aorta clearly show that the distance between both structures is greatest cranially and smallest caudally, and the difference becomes more pronounced with development. The boxed schematic drawings reveal that the most pronounced regional growth differences in the thoracic region (top row of rectangles) are present in the area between the bilateral sympathetic trunks on the one hand and the vertebrae (orange-coded triangles) or dorsal aorta (green-coded triangles) on the other hand. In fact, the base of the orange-coded triangle became ~2.5-fold wider between CS15 and CS21 in the thoracic area ("CC" in Figure 7D), but hardly increased in height in this period ("BE" in Figure 7C). After CS21, however, its height dropped dramatically to negative values in the thoracic area, which shows that the sympathetic trunks were acquiring a more dorsal position than the notochord. In contrast, the height of the orange-coded triangle remained unchanged in the lumbar and sacral area (Figure 7C). The green-coded triangle starts out with negative values because of the para-aortic position of the trunks, but increases steadily, in particular in the thoracic region. If the medial sacral artery can be taken as

the caudal continuation of the dorsal aorta, the sympathetic trunks in front of the sacrum (bottom row of rectangles) maintain their original para-aortic position throughout life. The scheme, finally, indicates that the vertebrae grow, but the growth spurt after the 8th week of development has no effect on the topographical position of the sympathetic trunks.

5 | CONCLUSION

Neural crest cells initially migrate and then form diffusely distributed sympathetic trunks in a para-aortic position. Differential growth of structures surrounding the sympathetic trunks then relocates the position of the sympathetic trunks to pre- or paravertebral. Simultaneously, the diffuse sympathetic ganglionic cells aggregate into ganglia with relatively ganglionic cell-free stretches in between.

CONFLICT OF INTERESTS

The authors declare that they have no competing interests.

ACKNOWLEDGEMENTS

The authors thank Drs Maurice van den Hoff (AMC), Marco de Ruyter (LUMC), and Annelieke Schepens (Radboud) for allowing us to use their institutional series of human embryos and fetuses. The authors thank Dr John Cork (Cell Biology & Anatomy, LSU Health Sciences Center, New Orleans) for making additional digitised sections of the Virtual Human Embryo project available to us. The authors also thank Dr Christoph Viebahn (Institute of Anatomy and Embryology, University Medical Center Göttingen, Göttingen) for allowing us to investigate digitised sections of the Blechschmidt Collection. The financial support of 'Stichting Rijn' is gratefully acknowledged. Special thanks goes to Els Terwindt (Maastricht University) and Corrie de Gier-de Vries (AMC) for technical assistance.

AUTHORS' CONTRIBUTIONS

N.K. was responsible for data collection, analysis and visualisation, and wrote the manuscript. J.H. and C.H. participated in data collection, analysis and interpretation. G.M. and N.K. were responsible for processing all Amira reconstructions in Cinema4D. S.E.K. participated in data analysis and interpretation, provided guidance, and edited the manuscript. W.H.L. conceived the study, provided guidance, assisted with data interpretation, and preparation of the manuscript.

ORCID

Nutmethee Kruepunga  <https://orcid.org/0000-0002-3871-1209>

Jill P. J. M. Hikspoors  <https://orcid.org/0000-0003-2940-1812>

S. Eleonore Köhler  <https://orcid.org/0000-0003-1977-9977>

Wouter H. Lamers  <https://orcid.org/0000-0003-3032-7824>

REFERENCES

- Andres KH, Kautzky R (1955) Early development of the cervical and cranial autonomic ganglia in man. *Zeitschrift für Anatomie und Entwicklungsgeschichte* 119, 55–84.
- Chan, W.H., Anderson, C.R. & Gonsalvez, D.G. (2018) From proliferation to target innervation: signaling molecules that direct sympathetic nervous system development. *Cell and Tissue Research*, 372, 171–193.
- Cochard, P., Goldstein, M. & Black, I.B. (1979) Initial development of the noradrenergic phenotype in autonomic neuroblasts of the rat embryo in vivo. *Developmental Biology*, 71, 100–114.
- Fernholm, M. (1971) On the development of the sympathetic chain and the adrenal medulla in the mouse. *Zeitschrift für Anatomie und Entwicklungsgeschichte*, 133, 305–317.
- Frick, H. (1949) Über den Abschluß der Verbindung zwischen Pleura und Perikard bei menschlichen Embryonen. *Z Anat Entwickl geschichte*, 114, 230–241.
- Furlan, A. & Adameyko, I. (2018) Schwann cell precursor: a neural crest cell in disguise? *Developmental Biology*, 444, S25–S35.
- Furlan, A., Dyachuk, V., Kastrioti, M.E. et al. (2017) Multipotent peripheral glial cells generate neuroendocrine cells of the adrenal medulla. *Science*, 357(6346), eaal3753.
- Gammill, L.S. & Roffers-Agarwal, J. (2010) Division of labor during trunk neural crest development. *Developmental Biology*, 344, 555–565.
- Gibbins, I. (1994) Comparative anatomy and evolution of the autonomic nervous system. In: Nilsson, S. and Holmgren, S. (Eds.) *Comparative physiology and evolution of the autonomic nervous system*. Chur, Switzerland: Harwood Academic Publisher, pp. 1–68.
- Goldstein, R.S. & Kalcheim, C. (1991) Normal segmentation and size of the primary sympathetic ganglia depend upon the alternation of rostrocaudal properties of the somites. *Development*, 112, 327–334.
- Groen, G.J., Baljet, B., Boekelaar, A.B. & Drukker, J. (1987) Branches of the thoracic sympathetic trunk in the human fetus. *Anatomy and embryology*, 176, 401–411.
- His Sr W (1890) Histogenese und Zusammenhang der Nerven-elemente. *Arch. f. Anat. u. Physiol. Anat. Abt.*, 97–117.
- Huber, K. (2006) The sympathoadrenal cell lineage: Specification, diversification, and new perspectives. *Developmental Biology*, 298, 335–343.
- Kameda, Y. (2014) Signaling molecules and transcription factors involved in the development of the sympathetic nervous system, with special emphasis on the superior cervical ganglion. *Cell and Tissue Research*, 357, 527–548.
- Kasemeier-Kulesa JC, Kulesa PM, Lefcort F (2005) Imaging neural crest cell dynamics during formation of dorsal root ganglia and sympathetic ganglia. *Development* 132, 235–45.
- Kasemeier-Kulesa, J.C., Morrison, J.A., Lefcort, F. & Kulesa, P.M. (2015) TrkB/BDNF signalling patterns the sympathetic nervous system. *Nature Communications*, 6, 8281.
- Kruepunga, N., Hikspoors, J., Hülsman, C.J.M., Mommen, G.M.C., Köhler, S.E. & Lamers, W.H. (2020a) Development of extrinsic innervation in the abdominal intestines of human embryos. *Journal of Anatomy*, 237, 655–671.
- Kruepunga, N., Hikspoors, J., Hülsman, C.J.M., Mommen, G.M.C., Köhler, S.E. & Lamers, W.H. (2020b) Extrinsic innervation of the pelvic organs in the lesser pelvis of human embryos. *Journal of Anatomy*, 237, 672–688.
- Kulesa, P.M., Lefcort, F. & Kasemeier-Kulesa, J.C. (2009) The migration of autonomic precursor cells in the embryo. *Autonomic Neuroscience*, 151, 3–9.
- Kuntz A (1910) The development of the sympathetic nervous system in mammals. *Journal of Comparative Neurology and Psychology* 20, 211–258.
- Kuntz, A. (1920) The development of the sympathetic nervous system in man. *Journal of Comparative Neurology*, 32, 173–229.
- Lumb, R. & Schwarz, Q. (2015) Sympathoadrenal neural crest cells: The known, unknown and forgotten? *Development, Growth & Differentiation*, 57, 146–157.
- Lutz, G. (1968) Die Entwicklung des Halssympathicus und des Nervus vertebralis. *Zeitschrift für Anatomie und Entwicklungsgeschichte*, 127, 187–200.

- Mekonen, H.K., Hikspoors, J.P., Mommen, G., Köhler, S.E. & Lamers, W.H. (2015) Development of the ventral body wall in the human embryo. *Journal of Anatomy*, 227, 673–685.
- Mekonen, H.K., Hikspoors, J.P., Mommen, G., Kruepunga, N., Köhler, S.E. & Lamers, W.H. (2017) Closure of the vertebral canal in human embryos and fetuses. *Journal of Anatomy*, 231, 260–274.
- Norden, J., Grieskamp, T., Lausch, E. et al. (2010) Wt1 and retinoic acid signaling in the subcoelomic mesenchyme control the development of the pleuropericardial membranes and the sinus horns. *Circulation Research*, 106, 1212–1220.
- Okuno, K., Ishizu, K., Matsubayashi, J. et al. (2019) Rib cage morphogenesis in the human embryo: A detailed three-dimensional analysis. *Anatomical Record (Hoboken)*, 302, 2211–2223.
- O'Rahilly, R. & Müller, F. (2007) The development of the neural crest in the human. *Journal of Anatomy*, 211, 335–351.
- O'Rahilly, R. & Muller, F. (2010) Developmental stages in human embryos: revised and new measurements. *Cells Tissues Organs*, 192, 73–84.
- Paterson, A.M. (1890) Development of the sympathetic nervous system mammals. *Philosophical Transactions of the Royal Society of London*, B., 181, 159.
- Pla, P. & Monsoro-Burq, A.H. (2018) The neural border: Induction, specification and maturation of the territory that generates neural crest cells. *Developmental Biology*, 444(Suppl 1), S36–S46.
- Pooh, R.K., Shiota, K. & Kurjak, A. (2011) Imaging of the human embryo with magnetic resonance imaging microscopy and high-resolution transvaginal 3-dimensional sonography: human embryology in the 21st century. *American Journal of Obstetrics and Gynecology*, 204, 77.e1–77.e16.
- Rothman, T.P., Gershon, M.D. & Holtzer, H. (1978) The relationship of cell division to the acquisition of adrenergic characteristics by developing sympathetic ganglion cell precursors. *Developmental Biology*, 65, 322–341.
- Rubin, E. (1985) Development of the rat superior cervical ganglion: ganglion cell maturation. *The Journal of Neuroscience*, 5, 673.
- Saito, D. & Takahashi, Y. (2015) Sympatho-adrenal morphogenesis regulated by the dorsal aorta. *Mechanisms of Development*, 138, 2–7.
- Salzer, G.M. (1960) Die Topogenese der Pleurahöhlen. *Z Anat Entwickl geschichte*, 122, 232–240.
- Streeter GL (1912) The Sympathetic Nervous System (part 4 of The Development of the Nervous system). In: *Manual of Human Embryology* (eds. Keibel F, Mall FP), pp. 144–156. Philadelphia: J.B. Lippincott Co..
- Theveneau, E. & Mayor, R. (2012) Neural crest delamination and migration: From epithelium-to-mesenchyme transition to collective cell migration. *Developmental Biology*, 366, 34–54.
- Vega-Lopez, G.A., Cerrizuela, S. & Aybar, M.J. (2017) Trunk neural crest cells: Formation, migration and beyond. *International Journal of Developmental Biology*, 61, 5–15.
- Woźniak, W., Grzymińska, M. & Lupicka, J. (2009) The first appearance of sympathetic ganglia in human embryos at stage 13. *Folia Morphol (Warsz)*, 68, 215–217.
- Wreite, M. (1959) The anatomy of the sympathetic trunks in man. *Journal of Anatomy*, 93, 448–459.

SUPPORTING INFORMATION

Additional supporting information may be found online in the Supporting Information section.

How to cite this article: Kruepunga N, Hikspoors JP, Hülsman CJ, Mommen GM, Köhler SE, Lamers WH. Development of the sympathetic trunks in human embryos. *J Anat.* 2021;239:32–45. <https://doi.org/10.1111/joa.13415>